**RSC Advances**

# Comparison between dispersive liquid–liquid microextraction and ultrasound-assisted nanoparticles-dispersive solid-phase microextraction combined with microvolume spectrophotometry method for the determination of Auramine-O in water samples

SCHOLARONE™
Manuscripts

1   **Comparison between dispersive liquid–liquid microextraction and ultrasound-assisted**
2   **nanoparticles-dispersive solid-phase microextraction combined with microvolume**
3   **spectrophotometry method for the determination of Auramine-O in water samples**
4
5   Arash Asfaram [a], Mehrorang Ghaedi[1a], Alireza Goudarzi [b], Mustafa Soylak [c]
6
7   [a] Chemistry Department, Yasouj University, Yasouj 75914-35, Iran.
8   [b] Department of Polymer Engineering, Golestan University, Gorgan, 49188-88369, Iran
9   [c] Erciyes University, Fen Fakultesi, Department of Chemistry, 38039 Kayseri, Turkey
10

11

12

13

14

15

16

17

18

19

20

21

22

23

24

25

26

27

28

[1] Corresponding author at: Tel.: +98 741 2223048; fax: +98 741 2223048.
E-mail address: m_ghaedi@mail.yu.ac.ir; m_ghaedi@yahoo.com (M. Ghaedi)

29    **Abstract**

30    Novel dispersive solid phase micro-extraction (DSPME) and dispersive liquid–liquid micro-

31    extraction (DLLME) protects combined with spectrophotometry designed for

32    preconcentration and/or determination of Auramine-O (AO) content in various real samples.

33    DSPME is based on the application of manganese dioxide nanoparticles loaded on activated

34    carbon ($MnO_2$-NPs-AC). This new material was fully identified and characterized with FT-

35    IR, FESEM, EDX and XRD analysis. Influence of variables different solid phase extraction

36    sorbents, type and volume of extracting solvent, sonication time, dispersive solvents,

37    centrifugation time and ionic strength (NaCl Concentration) on response properties were

38    optimized by Central Composite Design (CCD), response surface methodology (RSM) and

39    desirability function (DF) using STATISTICA. Optimum conditions was set for DSPME as 1

40    mg $MnO_2$-NPs-AC, 3 min sonication time and 100 µL Volume of extraction at pH 6.5, while

41    for DLLME conditions fixed at pH 6.5, 5 min centrifugation time, 0.035 mol $L^{-1}$ NaCl

42    concentration, 140, 1000 µL and 10 mL of extraction solvent ($CHCl_3$), disperser solvent

43    (Ethanol) and sample volume, respectively. Under optimum conditions, the method has linear

44    calibration curves over ranged from 10 to 1000 ng $mL^{-1}$ and 1-2000 ng $mL^{-1}$, with $R^2 = 0.9997$

45    for DLLME and 0.9998 for DSPME, while corresponding detection limits for DSPME and

46    DLLME more 2.836 ng $mL^{-1}$ and 0.232 ng $mL^{-1}$, respectively. The relative standard deviation

47    and enrichment factor were less than 4% (n= 10) and 99.93 for DLLME and 117.66 for

48    DSPME, respectively. The experimental results were compared with those obtained by use of

49    DLLME and DSPME. The procedures fully were applied for the preconcentration and

50    subsequent determination of AO in wastewater, tap water, rain water and river water.

51

52    **Keywords:** Auramine-O determination, Dispersive liquid–liquid micro-extraction, dispersive

53    solid-phase microextraction, Spectrophotometry.

## 1. Introduction

The sample matrix extensively affect the performance of each method especially in pollutant residue analysis in food samples. The removal of interference and matrix effect reduction as key part extensively effect accuracy, robust, and sensitivity of quantitative analysis [1, 2]. Auramine-O (diarylmethane dye, fluorescent stain) has yellow needle crystals with high solubility in water and ethanol. AO as stain acid-fast bacteria (e.g. Mycobacterium) agent binds to the mycolic acid in its cell wall similar to Ziehl-Neelsen stain [3]. It used as fluorescent version of Schiff reagent [4], while together with Rhodamine B act as Truant auramine-rhodamine stain for Mycobacterium tuberculosis [5, 6].

The cleanup is one of the consuming and labor intensive process to overcome matrix effects classified to solid phase extraction (SPE), gel permeation chromatography (GPC), dispersive liquid-liquid extraction (DLLE), liquid chromatography–mass spectrometry (LC–MS), voltammetry, Electrophoresis, chemiluminescence analysis, immuno analysis and dispersive solid phase extraction (DSPE), etcetera are widely used to overcome the matrix interferences [7-17]. Owing to the complexity of sample matrices and low levels of analytes preliminary, sample pretreatment and enrichment process assumed to be crucial steps of the analytical procedures. Conventional and widespread sample pretreatment methods such as liquid–liquid extraction [16], solid-phase extraction (SPE) [18, 19], liquid-phase microextraction [20], cloud point extraction [21], ionic liquids extraction [22] and stir bars microextraction [23] have their own a advantages and disadvantage. Most of these procedures suffer from drawbacks such as large amounts of organic solvent, tedious procedure or providing low enrichment factor. Liquid phase microextraction (hollow fiber based technique) as well as the stir bars microextraction in despite of their very low microliter organic solvent consumption possess relatively low recoveries and poor repeatability. Dispersive liquid–liquid microextraction (DLLME) [24, 25]. Based on the ternary component solvent system permit to achieve safe and

79    quantitative phase separation following formation of cloudy solution that simply achieved

80    following rapid injection of extraction and dispersive solvents into an aqueous sample

81    containing analytes.  The hydrophobic analytes simply enriched in the extraction solvent that

82    dispersed into the bulk aqueous solution, while their high interfacial surface area among

83    extraction and aqueous phase possible to achieve quantitative and quick extraction of the

84    analytes. After centrifugation, determination of the analytes in the settled phase can be

85    performed by conventional analytical techniques. The advantages of DLLME are simplicity

86    of operation, rapidity, low cost, low consumption of organic solvent, high recovery, high

87    enrichment factor and very short extraction time.  But the main disadvantage of DLLME is

88    consumption of third component (disperser organic solvent) which usually decreases analytes

89    partition coefficient among different phases. Recently, the dispersive solid-phase extraction

90    (DSPE) as popular clean-up procedure based on simple and facile sample extraction into

91    organic solvent that supply distinct advantages such as (quick, easy, chip, effective, rugged

92    and safe) [26] that is an extraction of Solid-phase  extraction  (SPE)  (reproducible  and  high

93    through put  capability) [27-30], while labor from his points such as  large  secondary wastes,  a

94    long  procedure  and  requirement of complex  equipment.  The  Dispersive solid phase micro-

95    extraction (DSMPE)  is superior to traditional  SPE in term of enhance in recoveries;  time

96    reduction and  decrease in solvent  consumption [31, 32], while supply  simple, economic and

97    easy protocol [33].  Appropriate selection of sorbents due to advantages such as presence of

98    reaction  centers  with  high  surface  area  lead  to  improve  in  methods  performances.

99    Applications of novel reactive and non-toxic nano-structure adsorbents that supply high

100    surface  area  and  reactive  centers  make  possible  to  improve  method  characteristic

101    performance. $MnO_2$-NPs-AC  as  an  extracting  phase  in  DSPME  was  used  and  offer

102    significantly  higher  surface  area-to-volume  ratio  that  associated  to  achievement  of  high

103    extraction capacity, rapid extraction dynamics and high extraction efficiencies.

104    In this study, for the first time, preparation of $MnO_2$ nanoparticles deposited on

105    activated carbon ($MnO_2$-NPs-AC) was reported and then the extraction efficiency of DLLME

106    and DSPME in combination with micro-volume spectrophotometry for AO analysis in water

107    samples were carried out using $MnO_2$-NPs-AC as an absorbent.    Influence of important

108    variables such as the sample pH, kind and volume of extraction and disperser solvent, salt

109    effect and extraction time were investigated and optimized by CCD and desirability function

110    (DF).

111

## 2.  Experimental

### 2.1.Reagents

114    All applied chemicals (analytical reagent grade) were supplied from Merck, Darmstadt,

115    Germany. Manganese sulfate dehydrate ($MnSO_4$, $2H_2O$) was used as manganese ion source

116    and purchased from Merck Company and used as received without further purification.

117    Ammonia solution (25 % w/w) as an oxygen source was provided from Chem. lab Company

118    and    used    as    received    without    further    purification.    Auramine-O    (4,    4-

119    dimethylaminobenzophenonimide) (AO), (Table 1) was supplied from Merck (Darmstadt,

120    Germany). A stock standard solution of AO (100 mg $L^{-1}$) was prepared in water and its

121    subsequent dilution was used as working solution.

122

### 2.2.Instrumentation

124    The absorbance was measured with a Perkin Elmer Lambda 25 spectrophotometer at a

125    wavelength of 429 nm using a quartz cell with an optical path of 1 cm. A Hermle

126    Labortechnik GmbH centrifuge model Z206A (Germany) was used to accelerate the phase

127    separation. A Metrohm digital pH-meter model 686 (Switzerland) with a combined Ag/AgCl

128    glass electrode was used for pH adjustments. X- ray diffraction (XRD, Philips PW 1800) was

129    performed to characterized the phase and structure of the prepared nanoparticles using Cu kα

130    radiation (40 kV and 30 mA) at angles ranging from 10 to $80^{\circ}$. The atomic composition of the

131    $MnO_2$-NPs-AC was analyzed by energy-dispersive X-ray spectrometer (EDX) using an

132    Oxford INCA II energy solid state detector. The morphology of the nanoparticles were

133    observed by field emission scanning electron microscopy (FESEM: Hitachi S4160) under an

134    acceleration voltage of 15 kV. To investigate the purity as well as the presence of organic

135    and/or other compounds in the prepared nanoparticles, a Fourier transform infrared (FT-IR)

136    spectrum was recorded using a Perkin Elmer-Spectrum RX-IFTIR spectrometer in the range

137    of 300–4000 $cm^{-1}$. An ultrasonic bath with heating system (Tecno-GAZ SPA Ultra Sonic

138    System) at 40 kHz of frequency and 130 W of power was used for the ultrasound-assisted

139    adsorption procedure. The STATISTICA, a statistical package software version 10.0 (Stat

140    Soft Inc., Tulsa, USA) was used for experimental design analysis and their subsequent

141    regression analysis. Statistical analysis of the model was performed to evaluate the analysis of

142    variance (ANOVA). The quality of the polynomial model equation was judged statistically by

143    the coefficient of determination $R^2$ and its statistical significance was determined by F-test. P-

144    values less than 0.05 were considered to be statistically significant.

145

146    *2.3.General procedure*

147    *2.3.1.   Dispersive liquid–liquid microextraction (DLLME)*

148       10 mL 0.035 mol $L^{-1}$ NaCl solution containing 500 ng $mL^{-1}$ of AO was placed in a 15.0 mL

149    screw cap glass test tube with conical bottom and its pH was adjusted 6.5. Mixture composed

150    of 1000 μL of ethanol (disperser solvent) and 140 μL $CHCl_3$ (extraction solvent) rapidly

151    injected into the above mentioned sample solution via a glass syringe and the mixture was

152    gently shaken. A cloudy solution of very fine droplets of $CHCl_3$ dispersed into aqueous

153    sample extensively and quantitatively extract the analytes into the fine droplets. Centrifuge of

154    mixture at 3000 rpm min$^{-1}$ for 5 min lead to setting and sedimentation of organic phase

155    (chloroform) at its bottom. Finally, 50 µL of the organic phase was removed by micro-syringe

156    and placed in a micro cell for determination of total AO by UV–Vis spectrophotometer (429

157    nm, Fig .1). The enrichment factor (EF) and extraction recovery (ER%) was estimated

158    according to literature [24].

159

160    *2.3.2.  Dispersive solid–phase microextraction (DSPME)*

161        At the sonochemical exposure possible to conduct the adsorption experiment in batch

162    mode as follows: 10 mL solution containing 500 ng mL$^{-1}$ of AO at pH 6.5 was mixed

163    thoroughly with 1 mg of MnO$_2$-NPs-AC in 15.0 mL screw cap glass test tube with conical

164    bottom at maintained the 3 min under exposure at the room temperature (298 K). The MnO$_2$-

165    NPs-AC containing the extracted analytes is finally separated from the sample matrix by

166    centrifugation (3000 rpm, 4 min) and subsequently the liquid phase was discarded using a

167    Pasteur pipette. In the next step, adsorbed analytes were eluted by 100 µL of acetone (as

168    desorption solvent). Finally, 50 µL of the organic phase was removed by micro-syringe and

169    placed in a micro cell for determination of total AO by UV–Vis spectrophotometer (429 nm,

170    Fig.1).

171

172    *2.4.Synthesis of MnO$_2$-NPs loaded on AC*

173        The MnO$_2$ nanoparticles loaded on activated carbon (MnO$_2$-NPs-AC) was prepared as

174    follows: first 12.5 gr activated carbon (AC) was mixed with 200 ml of 0.0125M manganese

175    sulfate solution as a deposition suspension solution in an Erlenmeyer flask. Then, 10 ml of

176    fresh ammonia solution (25 % w/w) was diluted by adding 50 ml distilled water in a beaker

177    and was added drop by drop to deposition solution along with strong stirring during 5 minutes

178    at 30$^{\circ}$C. Addition of diluted ammonia solution and vigorous mixing for 21 hours at room

179    temperature lead to obtain a homogenous deposition of $MnO_2$-NPs-AC. The suspension

180    solution of homogenous deposited $MnO_2$-NPs on activated carbon was heated at 65 $^{\circ}$C for one

181    hour. The obtained $MnO_2$-NPs-AC were filtered and washed several times by distilled water.

182    Finally the $MnO_2$-NPs loaded on AC were dried at 60 $^{\circ}$C for 3h and following characterized

183    and used as absorbent in adsorption experiments.

184

185    *2.5. Design of experiments*

186       Response surface methodology (RSM) as most prominent the optimization experimental

187    design [34] approach was used to estimate the main and interaction effect of variables. RSM

188    model and predict the relationship among controllable input parameters and the obtained

189    response surfaces [35] that supply a rapid, useful and efficient optimization protocol in

190    comparison to conventional, time consuming one factor-at-a-time approach [36]. In the present

191    study, central composite design (CCD) most abundant RSM branches was used for the

192    optimization of variables influence on preconcentration and determination of AO in water

193    samples.

194    The experimental data was analyzed by STATISTICA 10.0 software according to analysis of

195    variance (ANOVA) and a regression analysis follow the plotting response surface The

196    predicted values obtained from RSM model were compared with actual values for testing the

197    model. Finally, the experimental data obtained using the optimal specified conditions (Table

198    2) used as validating set and predicated response were compared with the predicted values.

199    The fitted quadratic response model is given by Eq. (1):

200

201    $$y = \beta_0 + \sum_{i=1}^{k}\beta_i x_i + \sum_{i=1}^{k}\sum_{j=1}^{k}\beta_{ij} x_i x_j + \sum_{i=1}^{k}\beta_{ii} x_i^2 + \varepsilon \qquad (1)$$

202

203    where y is the predicted response; $X_i$ and $X_j$ are the coded values of independent variables;

204    and $\beta_0$, $\beta_i$, $\beta_{ij}$ and $\beta_{ij}$ are the regression coefficients for intercept, linear, quadratic and

205    interaction terms, respectively. $\varepsilon$ represents the random error. Pareto chart was plotted using

206    STATISTICA 10.0 software, while the important effects are visually identified and the bars

207    are correspond to the absolute magnitudes of the estimated coefficients respect to each

208    variable. An effect exceeds the vertical line (p=0.05) indicate significant contribution of this

209    parameters on response.

210    To optimize the extraction conditions and verify their synergy and/or antagonism interaction

211    CCD for five variables at five levels (Table 2) at following specified conditions pH ($X_1$, 4.5-

212    8.5), extraction solvent volume ($X_2$, 50-250 µL), disperser solvent volume ($X_3$, 400-1200 µL),

213    centrifugation time ($X_4$, 2-6 min) and ionic strength ($X_5$, 0.0-0.06 mol $L^{-1}$) for the DLLME as

214    well as pH ($X_1$, 4.5-8.5), volume of extraction ($X_2$, 50-250 µL), adsorbent dosage ($X_3$, 0.5-2.5

215    mg), ultrasonic  time ($X_4$, 2-6 min) and ionic strength ($X_5$, 0.0-0.06 mol $L^{-1}$) for the DSPME

216    were selected as experimental factors.

217

218    **3.   Results and discussion**

219    *3.1.Characterization of adsorbent*

220       The size and morphology of the $MnO_2$-NPs loaded on AC was studied by field emission

221    scanning electron microscopy (FE-SEM) (Fig. 2(a)). FE- SEM image in Figure 2(a) reveals

222    that the $MnO_2$-NPs-AC was formed the sheet-like particles with thickness of about 50-100

223    nm, consist of many spherical-like nanoparticles with diameters of about 20-50 nm.

224    The chemical composition of the $MnO_2$-NPs loaded on AC was studied by EDX analysis and

225    confirmed the presence of Mn and O in the sample (Fig. 2(b)). The Au peak is related to the

226    signal detected from gold coating by sputtering during FE-SEM sample preparation. In EDX

227　analysis (Fig. 2b), C, O and Mn are the dominant elements throughout the surface of the

228　$MnO_2$-NPs-AC with weight percentages of 80.00%, 11.60%, and 8.40%, respectively.

229　The EDS mapping of the $MnO_2$-NPs-AC was presented in Fig. 2(c) in order to investigate

230　their localized elemental information. It is worth noting that the element of O and Mn were

231　well dispersed on the surface of adsorbent.

232　Figure 3(a) shows the XRD pattern of the $MnO_2$-NPs loaded on AC particles. The observed

233　broad hump at $2\theta$=20-25° as well as a broad peak at $2\theta$=43° is related to the amorphous nature

234　of activated carbon particles which $MnO_2$ nanoparticles loaded on them. Therefore, according

235　to the obtained XRD pattern the prepared $MnO_2$-NPs had an amorphous structure.

236　FT-IR spectrum of the prepared $MnO_2$-NPs-AC in the range of 300–4000 $cm^{-1}$ give useful

237　information about purity as well as the presence of organic and/or other compounds in

238　prepared $MnO_2$ nanoparticles (Fig. 3(b)). Hydroxides and oxides of metal nanoparticles

239　usually gives the absorption peak in the finger print region (<1000 $cm^{-1}$) due to inter-atomic

240　vibrations. An strong and sharp peak at 586 $cm^{-1}$ in the spectrum is due to Mn–O vibrations

241　modes in $MnO_2$ [37]. Jaganyi et al. [38] reported an absorption peak at 475 $cm^{-1}$ correspond to the

242　stretching collision of O–Mn–O, while peak at 458 $cm^{-1}$ is attributed to O–Mn–O bond. Broad

243　absorption peaks with maximum around 3381 $cm^{-1}$ and 1610 $cm^{-1}$ is assigned to water and/or

244　carbon dioxide adsorbed strongly on nanocrystalline materials with high surface-to-volume

245　ratio [39]. X. Chu et al. reported an absorption peak for the Mn-OH functional group at 1109

246　$cm^{-1}$. That has good agreement with FT-IR spectrum of the prepared $MnO_2$ nanoparticles. In

247　this work, no absorption peak related to the Mn-OH functional group was observed.

248

249　***3.2.****Central Composite Design (CCD)*

250　　The design matrix consist of 32 sets of experimental conditions in coded terms along with

251　their values and respective responses are given in Table 2. The recovery by CCD of AO by

252    DLLME and DSPME methods were in the range of 18.75% to 98.67% and 31.90% to

253    99.57%, respectively. The design suggest a second-order polynomial model for response of

254    both method and their sum of squares were presented in Table 3. The plot of experimental

255    results (Fig 4a) reveal the presence of linear relationship between them with high correlation

256    coefficient that indicates normal distribution of error around the mean and good applicability

257    of model for experimental data predication and supporting the normality assumption in fitted

258    model. The closeness ''Predicted'' and ''Adjusted R-Squared'' in addition to low and

259    acceptable standard deviation values (Table 3) confirm the suitability of predicate model for

260    the ratio for both DLLME and DSPME responses were 24.898 and 37.505 (respectively) is

261    greater than 4 and indicates adequacy of signal. Guan and Yao [40] suggested that $R^2$ should be

262    at least 0.80 for the good fit of a model. In this case, $R^2$ of the obtained model was 0.9863,

263    0.9935 for DLLME and DSPME, respectively. The sample variation of 98.63% and 99.35%

264    for %extraction recovery is attributed to the independent factors and only 1.36% and 0.65% of

265    the total variation are not explained by the model. This observation implied the proved

266    suitability and for the adequacy of model to representation of the actual relationship among

267    the selected factors.

268     Highly significant regression model is justified by higher Fischer's 'F statistics' values

269    with 'P' value (probability) as low as possible [41]. The Model F-value of 39.74 and

270    85.01  for DLLME and  DSPME support and confirm the significance of model  (Table  4).

271    The analysis of results by Pareto charts (P=95%) (Figs. 4b, c), reveal that the  terms  $X_1^2$,  $X_5$,

272    $X_3^2$,  $X_2X_3$,  $X_2X_5$ and $X_4X_5$ for DLLME, $X_2X_5$, $X_1$, $X_1^2$, $X_1X_3$, $X_3X_5$ and $X_5$ for DSPME were

273    significant, while other  remaining  terms  had less  significance and can be neglected. The

274    developed equation are as follows:

275

276
$$y_{DLLME} = -402 + 138.3X_1 + 0.6X_2 + 0.15X_3 - 1900X_5 + 0.1X_1X_2 - \\ 0.013X_1X_3 + 0.0005X_2X_3 - 1X_2X_5 + 0.7X_3X_5 + 202X_4X_5 \\ -11.6X_1^2 - 0.007X_2^2 - 0.000123X_3^2$$
(2)

277

278
$$y_{DSPME} = -31.6 + 78.8X_1 + 0.3X_2 - 120X_3 + 3.8X_1X_3 - 281X_1X_5 - \\ 0.058X_1X_2 - 774X_3X_5 + 7.8X_3X_4 + 0.33X_2X_3 + 5.14X_2X_5 + \\ 0.022X_2X_4 - 5.4X_1^2 + 4.64X_3^2 + 5826X_5^2 + 2.03X_4^2 - 0.002\,X_2^2$$
(3)

279

280   *3.3.Response surface methodology*

281      Response surfaces give good knowledge about interactions of variables and permit to

282   achieve optimal level of each variable that possible reaching the maximum response. Three-

283   dimensional response surfaces (Figs. 5 and 6). Indicate the effects of two factors on the %ER

284   at fixed and constant level of other variables (zero level). The 3-D plot (Fig. 5a), at above

285   condition confirm that the ER% increased and pH has positive relationship.

286   The 3-D plot (Fig. 5b) illustrates the interaction of the independent variables (extraction and

287   disperser solvents) on the response process. According to the 3D plot (Fig. 5b), highest AO

288   ER% was obtained at lower value of the disperser and extraction solvent volume. The

289   maximal ER% efficiency (over> 90%) was achieved at 140 μL CHCl$_3$ and 1000 μL of

290   extraction solvent at zero value of other variables.

291   The more the disperser solvent lead to reduce in extraction recovery efficiency, while higher

292   pH lead to better ER% efficiency (Fig. 5(c)).

293   Fig. 5(d) show the enhance in ER% by change in volume of extracting solvent from 40.0 to

294   140.0 and centrifugation time from 2 min to 4 min. The centrifugation time has positive

295   interaction with another variables temperature, while has apposite correlation disperser

296   solvent.

12

297   Fig.  6(a) shows response surface plot of the extraction recovery as dependent on pH and the

298   adsorbent dosage.  It seems necessary to mention the surface charge of $MnO_2$-NPs-AC in the

299   pH area under $pH_{ZPC}$ is positive, while suitable $H^+$ for adsorption and/or determination of

300   anionic compounds. In the pH area over $pH_{ZPC}$ the sorbent charge change to negative and

301   possible it as good and efficient it for removal of cationic compounds. In a low pH, $MnO_2$-

302   NPs-AC has positive charge and adsorb the negative charges compounds like anionic dyes at

303   pH over $pH_{ZPC}$, the oxide surface gets the negative charge and can make a complex with

304   cationic compounds.  According to above considerations, the basic conditions are more ideal

305   for AO dye adsorption and subsequent elution and determination.

306   Fig. 6(b) response the surface plot effect of adsorbent dosage and volume of extraction on the

307   ER%. Adsorbent dosage show negative linear effect and positive quadratic effect on the ER%

308   ($p < 0.000001$; $p < 0.03$). Volume of extraction has positive linear effect and negative quadratic

309   effect on the extraction recovery ($p < 0.00005$; $p < 0.002$). The ER% firstly increased and

310   subsequently raising the volume of extraction lead to reduce in ER%. 100 mL is favorable for

311   obtaining high ER% at lower adsorbent dosage.

312   The composed influence of volume of extraction and ultrasonic time on the ER by the

313   nanoparticles is shown in Fig.  6(c). It may be noted that the ER% reduce with increase in

314   ultrasonic time.

315   Fig. 6(d), in the middle value of each variable with respect to the ER% axial, the ER%

316   slightly increases and reach a plateau.

317

318   *3.4.Optimization of DLLME and DSPME conditions*

319        The determination of AO performances evaluated in terms of extraction recovery, which

320   largely varies with changes in variables. The extraction recovery was set at the highest value

321   as criteria. The model with good desirability was chosen and verified experimentally. The

322 optimized experimental conditions (Table 5) were used to study methods parameters. The

323 Table 5 confirm the closeness of predicted and experimental values. According to optimized

324 values predicted from model (Table 5) similar experiments were undertaken and was

325 validated with good agreement. Moreover, the extraction recovery has highest efficiency for

326 determination of AO by DSPME at 1 mg adsorbent dosage, 3 min sonication time, pH of 6.5

327 and 100 μL Volume of extraction, while in DLLME pH 6.5, 5 min centrifugation time, 0.035

328 mol L$^{-1}$ NaCl, 140, 1000 μL and 10 mL CHCl$_3$, Ethanol and sample volume, lead to

329 achievement of maximum characteristic performance. This was closer to optimized conditions

330 predicted by the model and confirms its usability for prediction of process behavior. Finally,

331 similar experiments were conducted and it was revealed that RSD lower than 4 % at predicted

332 optimum point confirm the adequate of model for real prediction of experimental date.

333

334 *3.5.Analytical figures of merit*

335 Several factors were evaluated to estimate the application of the proposed method for the

336 determination of AO in water samples (Table 6). The linear dynamic range for DLLME was

337 10–1000 ng mL$^{-1}$ and for DSPME was 1–2000 ng mL$^{-1}$. The correlation coefficient ($R^2$) was

338 higher than 0.999. Which indicate good linearity and applicability of method for AO

339 quantification. The ER% and EF were 99.77% and 99.34%, were 118 and 100 for DSPME

340 and DLLME, respectively. The lower detection limit (LOD) in both method was calculated

341 according to the IUPAC recommendation as follows: LOD $=KS_0/m$, where K is 3, $S_0$ is the

342 standard deviation of the blank (n= 10) and m is the slope of the respective calibration graph.

343 As it can seen, the DSPME and DLLME have detection limit of 0.232 ng mL$^{-1}$ and 2.836 ng

344 mL$^{-1}$, respectively.

345

346 *3.6. Study of interferences*

347       The determination of AO can be strongly affected by other constituents of samples. For

348   this reason, the selectivity of the presented methods was examined in the presence of possible

349   interfering ions and other dyes present in water samples. In these experiments, 10.0 mL of

350   solutions containing 500 ng mL$^{-1}$ AO and various amounts of diverse ions and dyes were

351   treated according to the recommended procedure. The tolerance limit are given in Table 7 (the

352   highest amount of diverse ions that produced an error not exceeding 5 %) investigation reveal

353   that majority of the investigated ions have no considerable influence on the AO

354   determination, while dyes presence in solution cause that the low tolerable limit was

355   observed. These results clearly demonstrated the moderate and selectivity of the developed

356   DLLME and DSPME for acceptable AO determination in water samples.

357

358   *3.7. Comparison of the presented procedure with other methods*

359       The figures of merit of DLLME and DSPME method for determination of AO in water

360   sample have been compared to earlier reported methods [42-53] (As shown in Table 8). The

361   comparison between DSPME and DLLME show that DSPME, is superior in term of lower

362   LOQ, higher linear dynamic range (LDR) and higher relative recoveries in comparison to

363   earlier methods and also DLLME. In addition, the extraction time in DSPME is shorter and

364   this method does not involve any labor-intensive and time consuming steps.

365

366   *3.8. Analysis of real samples and validity of the method*

367       The proposed methodology was applied to the speciation of AO in several water samples

368   including Tap water, river water, rain water, mineral water and wastewater were fur by

369   DLLME and DSPME combined with spectrophotometry (Table 9). The relative recovery of

370   the method was verified by the analysis of samples spiked with known amounts of AO. These

371    results demonstrated that the matrices of the studied water samples had little effect on

372    DLLME and DSPME for determination of AO.

373

374    **4.  Conclusion**

375         In   this   work,   comparison   between   DLLME   and   DSPME   combined   with

376    spectrophotometry for the determination of AO in water samples is proposed for the first

377    time. The experimental results indicate that trace levels of AO could be extracted from

378    aqueous   solutions   and   directly   determined   by   spectrophotometry.   Response   surface

379    methodology (RSM) combination with CCD model was used to examine the role of four

380    process variables on AO determination. The combination of CCD and desirability function

381    help us to obtain extraction recovery more than 95% at optimum conditions with RSD values

382    lower than 4% in all cases. A comparison of the proposed methods with the previously

383    reported methods for determination of AO (Table 9) indicates that the proposed methods

384    (DSPME) is high sensitivity, short analysis time, handling convenience and good accuracy. It

385    was successfully used in water samples, and the recovery was satisfactory.

386

390

391

392

393

394

**References:**

1.    C. Oellig and W. Schwack, *J. Chromatogr. A*, 2012, **1260**, 42-53.

2.    J. Hajšlová and J. Zrostlíková, *J. Chromatogr. A*, 2003, **1000**, 181-197.

3.    S. Kommareddi, C. R. Abramowsky, G. L. Swinehart and L. Hrabak, *Human pathology*, 1984, **15**, 1085-1089.

4.    T. Khavkin, M. Kudryavtseva, E. Dragunskaya, Y. Polotsky and B. Kudryavtsev, *Gastroenterology*, 1980, **78**, 782-790.

5.    J. Truant, W. Brett and W. Thomas Jr, *Henry Ford Hospital Medical Bulletin*, 1962, **10**, 287-296.

6.    M. Arrowood and C. Sterling, *J. Clin. Microbiol.*, 1989, **27**, 1490-1495.

7.    Q. G. Liao, Y. M. Zhou, L. G. Luo, L. B. Wang and X. H. Feng, *Microchim. Acta*, 2014, **181**, 163-169.

8.    B. Kanrar, S. Mandal and A. Bhattacharyya, *J. Chromatogr. A*, 2010, **1217**, 1926-1933.

9.    H. Abdolmohammad-Zadeh and Z. Talleb, *Microchim. Acta*, 2012, **179**, 25-32.

10.   W. Xie, C. Han, Y. Qian, H. Ding, X. Chen and J. Xi, *J. Chromatogr. A*, 2011, **1218**, 4426-4433.

11.   F. Calbiani, M. Careri, L. Elviri, A. Mangia, L. Pistara and I. Zagnoni, *J. Chromatogr. A*, 2004, **1042**, 123-130.

12.   M. Du, X. Han, Z. Zhou and S. Wu, *Food chem.*, 2007, **105**, 883-888.

13.   O. Chailapakul, W. Wonsawat, W. Siangproh, K. Grudpan, Y. Zhao and Z. Zhu, *Food Chem.*, 2008, **109**, 876-882.

14.   E. Mejia, Y. Ding, M. F. Mora and C. D. Garcia, *Food Chem.*, 2007, **102**, 1027-1033.

15.   Y. Zhang, Z. Zhang and Y. Sun, *J. Chromatogr. A*, 2006, **1129**, 34-40.

16.   Y. Wang, D. Wei, H. Yang, Y. Yang, W. Xing, Y. Li and A. Deng, *Talanta*, 2009, **77**, 1783-1789.

17.   T. Xu, K. Y. Wei, J. Wang, S. A. Eremin, S. Z. Liu, Q. X. Li and J. Li, *Anal. Biochem.*, 2010, **405**, 41-49.

18.   L. He, Y. Su, X. Shen, Z. Zeng and Y. Liu, *Anal. Chim. Acta.*, 2007, **594**, 139-146.

19.   Z. Zhang, H. Zhang, Y. Hu and S. Yao, *Anal. Chim. Acta.*, 2010, **661**, 173-180.

20.   F. J. López-Jiménez, S. Rubio and D. Pérez-Bendito, *Food chem.,* 2010, **121**, 763-769.

445
446  21.  W. Liu, W.-j. Zhao, J.-b. Chen and M.-m. Yang, *Anal. Chim. Acta.*, 2007, **605**, 41-45.
447
448  22.  Y. Fan, M. Chen, C. Shentu, F. El-Sepai, K. Wang, Y. Zhu and M. Ye, *Anal. Chim.*
449       *Acta.,* 2009, **650**, 65-69.
450
451  23.  C. Yu, Q. Liu, L. Lan and B. Hu, *J. Chromatogr. A.*, 2008, **1188**, 124-131.
452
453  24.  M. Rezaee, Y. Assadi, M.-R. Milani Hosseini, E. Aghaee, F. Ahmadi and S. Berijani,
454       *J. Chromatogr. A.*, 2006, **1116**, 1-9.
455
456  25.  A. V. Herrera-Herrera, M. Asensio-Ramos, J. Hernández-Borges and M. Á.
457       Rodríguez-Delgado, *TrAC, Trends Anal. Chem.*, 2010, **29**, 728-751.
458
459  26.  M. Anastassiades, S. J. Lehotay, D. Štajnbaher and F. J. Schenck, *J. AOAC Int.,* 2003,
460       **86**, 412-431.
461
462  27.  N. Li and H. K. Lee, *J. Chromatogr. A.*, 2001, **921**, 255-263.
463
464  28.  M. J. López de Alda and D. Barceló, *J. Chromatogr. A.*, 2001, **938**, 145-153.
465
466  29.  S. Rodriguez-Mozaz, M. J. López de Alda and D. Barceló, *J. Chromatogr. A.*, 2004,
467       **1045**, 85-92.
468
469  30.  K. Mitani, M. Fujioka and H. Kataoka, *J. Chromatogr. A.*, 2005, **1081**, 218-224.
470
471  31.  C. Basheer, H. G. Chong, T. M. Hii and H. K. Lee, *Anal. chem.,* 2007, **79**, 6845-6850.
472
473  32.  C. Basheer, A. A. Alnedhary, B. Rao and H. K. Lee, *J. Chromatogr. A.*, 2009, **1216**,
474       211-216.
475
476  33.  Y.-G. Zhao, X.-H. Chen, S.-D. Pan, H. Zhu, H.-Y. Shen and M.-C. Jin, *Talanta*, 2013,
477       **115**, 787-797.
478
479  34.  R. H. Myers, D. C. Montgomery and C. M. Anderson-Cook, *Response surface*
480       *methodology: process and product optimization using designed experiments*, John
481       Wiley & Sons, 2009.
482
483  35.  N. Aslan, *Powder Technol.*, 2008, **185**, 80-86.
484
485  36.  M. Alim, J.-H. Lee, C. Akoh, M.-S. Choi, M.-S. Jeon, J.-A. Shin and K.-T. Lee, *LWT-*
486       *Food Sci. Technol.*, 2008, **41**, 764-770.
487
488  37.  X. Chu and H. Zhang, *Modern Applied Science*, 2009, **3**, P177.
489
490  38.  D. Jaganyi, M. Altaf and I. Wekesa, *Appl Nanosci.*, 2013, **3**, 329-333.
491
492  39.  Y. C. Zhang, T. Qiao, X. Y. Hu and W. D. Zhou, *J. Cryst. Growth.*, 2005, **280**, 652-
493       657.
494

495 40. X. Guan and H. Yao, *Food Chem.*, 2008, **106**, 345-351.
496

497 41. A. I. Khuri and J. A. Cornell, *Response surfaces: designs and analyses*, CRC press,
498 1996.
499

500 42. L. Meizhong, *Sci. Technol. Food. Ind.*, 2005, **8**, 059.
501

502 43. L. Q. Z. X.-y. H. S.-k. D. M. X. Yong, *Food Science*, 2009, **30**, 194-196.
503

504 44. H.-q. ZHANG, L.-j. LIANG, Z.-y. HE and L.-k. SHI, *J. Chin. Mass. Spectrom. Soc.*,
505 2010, **1**, 012.
506

507 45. Z. Xiao-yan, *J. Anal. Sci.*, 2009, **4**, 010.
508

509 46. Z. Haiyuna, L. Jiangmeia, C. Zuanguangb, Z. Qinga and P. Yufanga, *Chin. J. Appl.*
510 *Chem.*, 2013, **4**, 023.
511

512 47. D.-q. LIN, C.-b. WAN, P. QIU and H.-m. LIU, *J. Chin. Mass. Spectrom. Soc.,* 2013,
513 **3**, 008.
514

515 48. Z. XiaoJun, Y. ChunRong, D. Can and X. ChunXiang, *J. Food Saf. and Qual.*, 2012,
516 **3**, 190-194.
517

518 49. J.-w. WANG, H.-j. ZHONG and C.-q. LIANG, *Anal. Test. Technol. Instrum.*, 2010, **2**,
519 013.
520

521 50. J. Li, H. Zhai, Z. Chen, Q. Zhou, Z. Liu and Z. Su, *J. Sep. Sci.*, 2013, **36**, 3608-3614.
522

523 51. C. Tatebe, X. Zhong, T. Ohtsuki, H. Kubota, K. Sato and H. Akiyama, *Food Science*
524 *& Nutrition*, 2014.
525

526 52. Z. Wang, L. Zhang, N. Li, L. Lei, M. Shao, X. Yang, Y. Song, A. Yu, H. Zhang and F.
527 Qiu, *J. Chromatogr. A.*, 2014, **1348**, 52-62.
528

529 53. C. Peng, Q. Xu-Guang, L. Xi-Shan, G. Jin-Pei, F. Jian and Z. Xi-Qing, *Chin. J. anal.*
530 *chem.*, 2011, **39**, 1670-1675.

531

532

533

534

535

536

537

538

539                                    **Figure captions:**

540    **Fig. 1.** The UV–Vis spectra of **(a)** blank solution (without dye), **(b)** before dispersive **(c)**

541    DLLME and **(d)** DSPME, respectively.

542

543    **Fig. 2**. (**a**) FE-SEM images of the prepared $MnO_2$-NPs-AC. (**b**) EDS analysis and (**c**) EDS

544    mapping of the $MnO_2$-NPs-AC adsorbent.

545

546    **Fig. 3.** (**a**) XRD pattern of the $MnO_2$ nanoparticles loaded on activated carbon. (**b**) FT-IR

547    spectrum of the prepared $MnO_2$ nanoparticles.

548

549    **Fig. 4. a**) The experimental data versus predicted data for DLLME and DSPME. **b**)

550    Standardized main effect Pareto chart for the central composite design of DSPME and **c**)

551    Standardized main effect Pareto chart for the central composite design of DLLME**.**

552

553    **Fig. 5.** Response surface plots for combined effect of Extraction solvent- pH (**a**),

554    Disperser solvent-Extraction solvent (**b**), pH-Disperser solvent (**c**) and Centrifugation time-

555    Extraction solvent (**d**) on the ER% of AO by DLLME.

556

557    **Fig. 6.** Response surface plots for combined effect of Adsorbent dosage- pH (**a**),

558    Adsorbent dosage–Volume of extraction (**b**), Volume of extraction - ultrasonic time (**c**) and

559    Volume of extraction - pH (**d**) on the ER% of AO by DSPME.

560
561
562
563
564
565
566
567
568
569
570
571
572
573
574

**Table captions:**

576 **Table 1.** Properties of the dye.

577

578 **Table 2.** Design matrix for the central composite designs.

579

580 **Table 3.** Model summary statistics and quality of quadratic model based on $R^2$ and standard

581 deviation for determination of AO in water samples.

582

583 **Table 4.** Analysis of variance (ANOVA) for determination of AO in water samples.

584

585 **Table. 5.** Optimum conditions derived by RSM design for determination of AO in water

586 samples (N=6).

587

588 **Table 6.** Analytical characteristics of the proposed methods.

589

590 **Table 7.** Tolerance limits of interfering species in the determination of 500 ng mL$^{-1}$ AO by

591 DLLME and DSPME methods.

592

593 **Table 8.** Comparison of the published methods with the proposed methods in this work.

594

595 **Table 9**. Extraction recoveries and RSD in different water samples at spiked level by the

596 DLLME and DSPME methods (N=3).

597

598

599

600

601

602

603

604

605
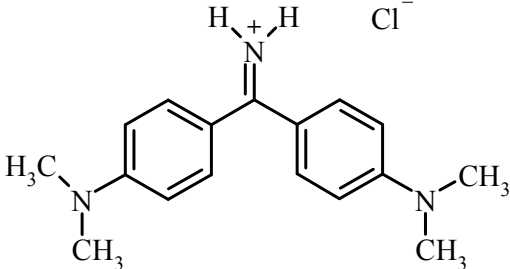
606

607

608

609

610    **Table 1.**
611        Properties of the dyes

| Properties | Auramine-O (AO) |
|---|---|
| Color index number | 41000 |
| CAS number | 2465-27-2 |
| Chemical Formula | $C_{17}H_{21}N_3.HCl$ |
| Molecular weight (g mol$^{-1}$) | 303.83 |
| Maximum wavelength ($\lambda_{max}$), nm | 429 |
| chemical structure | |
| Type of dye | Basic Yellow (Cationic) |
| Use | paper mills, textile mills, leather and carpet industry |



612

613

614

615

616

617

618

619

620

621

622

623

624

625

626

627

628

629

630

631

632

633

634

635

636

637

638

639 **Table 2.**
640 Design matrix for the central composite designs.

| Factors | Levels | | | | |
|---|---|---|---|---|---|
| | -α | Low (-1) | Central (0) | High (+1) | +α |
| $X_1$: pH | 4.5 | 5.5 | 6.5 | 7.5 | 8.5 |
| $X_2$: Extraction solvent [a] (µL) (Chloroform) | 50 | 100 | 150 | 200 | 250 |
| $X_2$: Volume of extraction [b] (µL) (Acetonitrile) | 50 | 100 | 150 | 200 | 250 |
| $X_3$: Disperser solvent (µL)[a] (Ethanol) | 400 | 600 | 800 | 1000 | 1200 |
| $X_3$: adsorbent dosage (mg)[b] ($MnO_2$-NP-AC) | 0.5 | 1 | 1.5 | 2 | 2.5 |
| $X_4$: Centrifugation time (min)[a] | 2 | 3 | 4 | 5 | 6 |
| $X_4$: Ultrasonic time (min)[b] | 2 | 3 | 4 | 5 | 6 |
| $X_5$: Ionic strength (NaCl concentration) (mol $L^{-1}$) | 0 | 0.015 | 0.03 | 0.045 | 0.06 |

| Run | $X_1$ | | $X_2$ | | $X_3$ | | $X_4$ | | $X_5$ | | ER%[a] AO | ER%[b] AO |
|---|---|---|---|---|---|---|---|---|---|---|---|---|
| | a | b | a | b | a | b | a | b | a | b | Observed | Observed |
| 1 | 5.5 | 7.5 | 100 | 100 | 600 | 1.0 | 5 | 5 | 0.015 | 0.045 | 69.44 | 87.46 |
| 2 | 7.5 | 7.5 | 200 | 100 | 600 | 1.0 | 3 | 3 | 0.045 | 0.015 | 18.75 | 99.51 |
| 3 | 6.5 | 7.5 | 50 | 100 | 800 | 2.0 | 4 | 3 | 0.030 | 0.045 | 40.21 | 31.90 |
| 4 | 6.5 | 7.5 | 150 | 200 | 400 | 1.0 | 4 | 5 | 0.030 | 0.015 | 62.47 | 56.80 |
| 5 | 6.5 | 5.5 | 150 | 100 | 800 | 2.0 | 4 | 5 | 0.030 | 0.045 | 87.15 | 38.52 |
| 6 | 5.5 | 6.5 | 200 | 150 | 600 | 1.5 | 3 | 4 | 0.015 | 0.000 | 28.12 | 76.49 |
| 7 | 5.5 | 5.5 | 100 | 100 | 600 | 1.0 | 3 | 5 | 0.045 | 0.015 | 60.83 | 71.86 |
| 8 | 6.5 | 6.5 | 150 | 150 | 800 | 1.5 | 4 | 4 | 0.030 | 0.030 | 94.10 | 69.73 |
| 9 | 5.5 | 8.5 | 200 | 150 | 1000 | 1.5 | 5 | 4 | 0.015 | 0.030 | 68.76 | 52.31 |
| 10 | 4.5 | 6.5 | 150 | 150 | 800 | 1.5 | 4 | 4 | 0.030 | 0.030 | 52.69 | 72.82 |
| 11 | 5.5 | 7.5 | 100 | 200 | 1000 | 2.0 | 5 | 3 | 0.045 | 0.015 | 87.33 | 61.56 |
| 12 | 6.5 | 6.5 | 150 | 150 | 1200 | 1.5 | 4 | 4 | 0.030 | 0.030 | 80.44 | 71.11 |
| 13 | 7.5 | 6.5 | 200 | 150 | 1000 | 1.5 | 3 | 4 | 0.015 | 0.030 | 39.19 | 68.65 |
| 14 | 6.5 | 6.5 | 150 | 150 | 800 | 2.5 | 4 | 4 | 0.030 | 0.030 | 83.36 | 49.16 |
| 15 | 5.5 | 7.5 | 200 | 100 | 600 | 2.0 | 5 | 5 | 0.045 | 0.015 | 31.28 | 71.14 |
| 16 | 6.5 | 6.5 | 150 | 150 | 800 | 1.5 | 4 | 6 | 0.030 | 0.030 | 84.38 | 79.32 |
| 17 | 7.5 | 5.5 | 100 | 100 | 600 | 2.0 | 5 | 3 | 0.045 | 0.015 | 55.65 | 46.40 |
| 18 | 6.5 | 6.5 | 150 | 50 | 800 | 1.5 | 6 | 4 | 0.030 | 0.030 | 98.67 | 51.69 |
| 19 | 7.5 | 6.5 | 100 | 150 | 600 | 0.5 | 3 | 4 | 0.015 | 0.030 | 56.69 | 98.21 |
| 20 | 6.5 | 5.5 | 150 | 100 | 800 | 1.0 | 4 | 3 | 0.000 | 0.045 | 96.83 | 93.03 |
| 21 | 8.5 | 5.5 | 150 | 200 | 800 | 2.0 | 4 | 5 | 0.030 | 0.015 | 36.42 | 57.95 |
| 22 | 6.5 | 5.5 | 150 | 200 | 800 | 1.0 | 4 | 5 | 0.060 | 0.045 | 83.64 | 81.82 |
| 23 | 6.5 | 5.5 | 150 | 200 | 800 | 2.0 | 4 | 3 | 0.030 | 0.045 | 88.89 | 51.38 |
| 24 | 7.5 | 4.5 | 100 | 150 | 1000 | 1.5 | 5 | 4 | 0.015 | 0.030 | 52.69 | 42.82 |
| 25 | 7.5 | 7.5 | 200 | 200 | 600 | 2.0 | 5 | 5 | 0.015 | 0.045 | 37.36 | 61.73 |
| 26 | 5.5 | 7.5 | 200 | 200 | 1000 | 1.0 | 3 | 3 | 0.045 | 0.045 | 39.19 | 67.10 |
| 27 | 5.5 | 6.5 | 100 | 250 | 1000 | 1.5 | 3 | 4 | 0.015 | 0.030 | 73.42 | 43.02 |
| 28 | 7.5 | 6.5 | 100 | 150 | 1000 | 1.5 | 3 | 4 | 0.045 | 0.030 | 44.86 | 74.18 |
| 29 | 7.5 | 6.5 | 200 | 150 | 1000 | 1.5 | 5 | 4 | 0.045 | 0.060 | 68.76 | 72.09 |
| 30 | 6.5 | 6.5 | 150 | 150 | 800 | 1.5 | 2 | 2 | 0.030 | 0.030 | 74.06 | 75.00 |
| 31 | 6.5 | 5.5 | 150 | 200 | 800 | 1.0 | 4 | 3 | 0.030 | 0.015 | 85.83 | 62.28 |
| 32 | 6.5 | 6.5 | 250 | 150 | 800 | 1.5 | 4 | 4 | 0.030 | 0.045 | 69.44 | 70.08 |

641 [a] DLLME.
642 [b] DSPME.

643 **Table 3.**

644 Model summary statistics and Quality of quadratic model based on $R^2$ and standard deviation for determination of AO in water samples.

Model Summary Statistics

| | | | DLLME | | | | | DSPME | | | |
|---|---|---|---|---|---|---|---|---|---|---|---|
| | | | $R^2$ | $R^2$ | | | | $R^2$ | $R^2$ | | |
| Source | SD | $R^2$ | Adjusted | Predicted | PRESS | SD | $R^2$ | Adjusted | Predicted | PRESS | |
| Linear | 23.130 | 0.2699 | 0.1294 | -0.06375 | 20256 | 13.540 | 0.4600 | 0.3530 | 0.113188 | 7782.12 | |
| 2FI | 27.823 | 0.3497 | -0.2600 | -4.44866 | 103755 | 11.430 | 0.7620 | 0.5390 | 0.572106 | 3754.939 | |
| Quadratic | 4.861 | 0.9864 | 0.9620 | 0.754547 | 4674 | 2.280 | 0.9940 | 0.9820 | 0.903281 | 848.744 | Suggested |
| Cubic | 5.390 | 0.9910 | 0.9530 | -4.66634 | 107900 | 3.047 | 0.9940 | 0.9670 | -3.23221 | 37139.31 | Aliased |

Quality of quadratic model based on $R^2$ and standard deviation

| Response | SD | mean | CV% | Adequate precision |
|---|---|---|---|---|
| DLLME | 4.861 | 62.030 | 7.84 | 24.898 |
| DSPME | 2.28 | 66.12 | 3.45 | 37.505 |

645
646
647
648
649
650
651
652
653
654
655
656
657
658
659
660
661

662 **Table 4.**

663 Analysis of variance (ANOVA) for determination of AO in water samples.

| Method | DLLME | | | | | DSPME | | | | |
|---|---|---|---|---|---|---|---|---|---|---|
| Factor | SS[a] | Df[b] | MS[c] | F-value | P-value | SS[a] | Df[b] | MS[c] | F-value | P-value |
| Model | 18782.28 | 20 | 939.1141 | 39.73472 | < 0.0001 | 8718.313 | 20 | 435.9156 | 84.00517 | < 0.0001 |
| $X_1$ | 570.08 | 1 | 570.077 | 38.0087 | 0.001634 | 117.793 | 1 | 117.793 | 27.3731 | 0.003376 |
| $X_1^2$ | 3912.69 | 1 | 3912.691 | 260.8707 | 0.000017 | 854.717 | 1 | 854.717 | 198.6210 | 0.000032 |
| $X_2$ | 2460.09 | 1 | 2460.094 | 164.0218 | 0.000052 | 134.312 | 1 | 134.312 | 31.2118 | 0.002535 |
| $X_2^2$ | 8705.71 | 1 | 8705.707 | 580.4354 | 0.000002 | 871.404 | 1 | 871.404 | 202.4988 | 0.000031 |
| $X_3$ | 963.12 | 1 | 963.124 | 64.2144 | 0.000489 | 3715.246 | 1 | 3715.246 | 863.3567 | 0.000001 |
| $X_3^2$ | 682.51 | 1 | 682.514 | 45.5053 | 0.001086 | 39.480 | 1 | 39.480 | 9.1744 | 0.029117 |
| $X_4$ | 85.93 | 1 | 85.934 | 5.7295 | 0.062108 | 21.805 | 1 | 21.805 | 5.0672 | 0.074180 |
| $X_4^2$ | 0.49 | 1 | 0.490 | 0.0326 | 0.863713 | 120.924 | 1 | 120.924 | 28.1007 | 0.003189 |
| $X_5$ | 1059.31 | 1 | 1059.309 | 70.6273 | 0.000391 | 22.873 | 1 | 22.873 | 5.3153 | 0.069296 |
| $X_5^2$ | 35.36 | 1 | 35.361 | 2.3576 | 0.185266 | 50.396 | 1 | 50.396 | 11.7112 | 0.018794 |
| $X_1X_2$ | 378.71 | 1 | 378.708 | 25.2496 | 0.004018 | 135.830 | 1 | 135.830 | 31.5645 | 0.002473 |
| $X_1X_3$ | 110.12 | 1 | 110.119 | 7.3419 | 0.042296 | 57.458 | 1 | 57.458 | 13.3521 | 0.014686 |
| $X_1X_4$ | 33.60 | 1 | 33.600 | 2.2402 | 0.194720 | 25.185 | 1 | 25.185 | 5.8525 | 0.060178 |
| $X_1X_5$ | 0.01 | 1 | 0.005 | 0.0003 | 0.985979 | 283.449 | 1 | 283.449 | 65.8685 | 0.000461 |
| $X_2X_3$ | 448.65 | 1 | 448.645 | 29.9125 | 0.002783 | 1040.670 | 1 | 1040.670 | 241.8332 | 0.000020 |
| $X_2X_4$ | 8.82 | 1 | 8.822 | 0.5882 | 0.477757 | 20.056 | 1 | 20.056 | 4.6607 | 0.083306 |
| $X_2X_5$ | 166.36 | 1 | 166.356 | 11.0915 | 0.020770 | 237.952 | 1 | 237.952 | 55.2959 | 0.000693 |
| $X_3X_4$ | 60.81 | 1 | 60.808 | 4.0542 | 0.100197 | 242.796 | 1 | 242.796 | 56.4214 | 0.000662 |
| $X_3X_5$ | 166.11 | 1 | 166.106 | 11.0748 | 0.020827 | 538.858 | 1 | 538.858 | 125.2209 | 0.000099 |
| $X_4X_5$ | 147.30 | 1 | 147.302 | 9.8211 | 0.025845 | 91.594 | 1 | 91.594 | 21.2849 | 0.005769 |
| Lack-of-Fit | 184.99 | 6 | 30.831 | 2.0556 | 0.223171 | 35.564 | 6 | 5.927 | 1.3774 | 0.371276 |
| Pure Error | 74.99 | 5 | 14.999 | | | 21.516 | 5 | 4.303 | | |
| Total | 19042.26 | 31 | | | | 8775.393 | 31 | | | |

664 [a] Sequential sums of squares
665 [b] Degrees of freedom
666 [c] mean sums of squares

667 **Table 5.**

668 Optimum conditions derived by RSM design for determination of AO in water samples (N=6).

| Variables | X$_1$ | X$_2$ | X$_3$ | X$_4$ | X$_5$ | Observed value [a] | Predicted value [b] |
|---|---|---|---|---|---|---|---|
| | | | Optimal conditions | | | ER% | |
| DLLME | 6.5 | 140 μL | 1000 μL | 5 min | 0.035 | 97.22±3.43 | 99.4 |
| DSPME | 6.5 | 100 μL | 1.0 mg | 3.0 min | 0.000 | 98.42±2.10 | 100 |

669 [a] Experimental values of response.

670 [b] Predicted values of response by RSM proposed model.

671

672

673

674

675

676

677

678

679

680

681

682

683

684

685

686

687     **Table 6**.
688     Analytical characteristics of the proposed methods.

| Quantitative analysis | DLLME | DSPME |
|---|---|---|
| Regression equation before preconcentration | y = 0.054x + 0.006,     R² = 0.9999 | |
| Regression equation after preconcentration | y = 5.396x + 0.613,     R² = 0.9998 | y = 6.353x + 0.163,     R² = 0.9997 |
| Sample volume (mL) | 10 | 10 |
| Volume Extraction solvent (µL) | 140 | 100 |
| Linear range (ng mL$^{-1}$) | 10-1000 | 1-2000 |
| Limit of detection (LOD) (ng mL$^{-1}$) | 2.836 | 0.232 |
| Reproducibility (RSD, %) | 3.207 | 1.518 |
| Repeatability (RSD, %) (N=10) | 3.958 | 2.268 |
| Average Recoveries (%) in samples at spiked | 94.573 | 97.436 |
| limit of quantification (LOQ) (ng mL$^{-1}$) | 9.452 | 0.772 |
| preconcentration factor | 71.430 | 100 |
| Enrichment factor | 99.930 | 117.662 |

689
690
691
692
693
694
695
696
697
698
699
700
701
702

703 **Table 7.**

704 Tolerance limits of interfering species in the determination of 500 ng mL$^{-1}$ AO by DLLME and DSPME

705 methods.

| Interference | Tolerance ratio ($\mu$g mL$^{-1}$) | | Added as |
|---|---|---|---|
| | DLLME | DSPME | |
| $Cu^{2+}$ | 1500 | 1000 | $Cu(NO_3)_2$ |
| $NH_4^+$ | 500 | 1000 | $NH_4NO_3$ |
| $CO^{2+}$ | 1000 | 500 | $Co(NO_3)_2$ |
| $Ni^{2+}$ | 500 | 500 | $Ni(NO_3)_2$ |
| $Cr^{2+}$ | 500 | 2000 | $Cr(NO_3)_3$ |
| $Ca^{2+}$ | 1200 | 1500 | $Ca(NO_3)_2$ |
| $Ba^{2+}$ | 1000 | 1500 | $Ba(NO_3)_2$ |
| $Pb^{2+}$ | 500 | 1000 | $Pb(NO_3)_2$ |
| $Zn^{2+}$ | 1500 | 2000 | $Zn(NO_3)_2$ |
| K+ | 1500 | 2000 | $KNO_3$ |
| $Mg^{2+}$ | 1200 | 2000 | $Mg(NO_3)_2$ |
| $Ag^+$ | 1200 | 1500 | $AgNO_3$ |
| $Na^+$ | 1200 | 2000 | $NaNO_3$ |
| $Ba^{2+}$ | 800 | 1500 | $Ba(NO_3)_2$ |
| $Fe^{2+}$ | 2000 | 2000 | $Fe(NO_3)_2$ |
| $Cl^-$ | 2000 | 2000 | NaCl |
| $F^-$ | 1000 | 1500 | NaF |
| Tartrazine, Sunset Yellow FCF | 100 | 50 | |
| Allura Red AC, Ponceau 4R | 90 | 40 | |
| Carmoisine | 80 | 40 | |

706

707

708

709

710

711

712

713

714

715

716

717

718

719    **Table 8.**
720    Comparison of the published methods with the proposed methods in this work.

| Dye | method | Correlation coefficient | Recoveries (%) | Precision (% RSD) | LOD (ng mL$^{-1}$) | LOQ (ng mL$^{-1}$) | Linear range (ng mL$^{-1}$) | Ref. |
|---|---|---|---|---|---|---|---|---|
| DLLME | HPLC-DAD[a] | 0.999 | 94.0-96.5 | 1.5 | - | - | 250- 50000 | 42 |
| | HPLC[b] | 0.998 | 72.3-96.5 | 0.3-8.8 | 30.0 | - | 0.50-2500 | 43 |
| | HPLC -ETMS[c] | 0.999 | 78.9- 92.1 | 11 | - | 0.5 | 2.5-100 | 44 |
| | UPLC-TMS[d] | 0.995 | 74.3- 91.1 | 2.4-9.4 | 0.30 | - | 10−500 | 45 |
| | MCE[e] | 0.999 | 95.5-96.2 | 2.6-3.0 | 20 | - | 5000-100000 | 46 |
| | HPLC-MS/MS[d] | 0.999 | 81.4-119 | 4.3-7.7 | 15 | 50 | 5-200 | 47 |
| | Spectrophotometric | 0.999 | 91.91-99.33 | 2.57-3.74 | 2.836 | 9.452 | 10-1000 | This work |
| DSPME | LC-TMS[f] | 0.999 | 84.2-95.1 | 4.5 | 1.0 | - | - | 48 |
| | UPLC-TMS[d] | 0.998 | 80.1-95.3 | - | 1.28 | 4.27 | - | 49 |
| | HPLC[b] | 0.999 | 90.5-92.4 | 2.1-4.4 | 17.85 | - | 250-25000 | 50 |
| | HPLC[b] | 0.999 | 70.2-92.7 | 3.7- 7.7 | 1.25 | 2.5 | 50-100000 | 51 |
| | IL-based MSPD–HLLME[g] | 0.998 | 98.23-103.54 | 3.9-5.9 | 6.7 | 13.4 | 20-1000 | 52 |
| | UPLC-TMS[d] | 0.999 | 72.6-90.2 | 3.8-5.6 | 0.48 | 1.6 | 1-100 | 53 |
| | Spectrophotometric | 0.999 | 95.99-99.77 | 1.30-3.30 | 0.232 | 0.772 | 1-2000 | This work |

721    [a] High performance liquid chromatography-diode array detector
722    [b] High Performance Liquid Chromatographic
723    [c] High- performance Liquid Chromatography-Electrospray Tandem Mass Spectrometry
724    [d] Ultra Performance Liquid Chromatography-Tandem Mass Spectrometry
725    [e] Microchip Capillary Electrophoresis
726    [f] Liquid Chromatography-Tandem Mass Spectrometry
727    [g] Ionic Liquid-based Matrix Solid-Phase Dispersion Homogeneous Liquid–Liquid Microextraction
728
729
730
731
732
733
734

735 **Table 9**.

736 Extraction recoveries and RSD in different water samples at spiked level by the DLLME and

737 DSPME methods (N=3).

| Samples | added (ng mL$^{-1}$) | | Found (ng mL$^{-1}$) | | ER% ± RSD (%) | |
|---|---|---|---|---|---|---|
| | DLLME | DSPME | DLLME | DSPME | DLLME | DSPME |
| Rain water | 500 | 500 | 478.95 | 479.93 | 95.79±3.50[a] | 95.99±1.92 |
| Tap water | 500 | 500 | 464.53 | 488.42 | 92.91±3.72 | 97.68±3.29 |
| Double-distilled water | 500 | 500 | 496.70 | 498.84 | 99.34±2.58 | 99.77±1.42 |
| Mineral water | 500 | 500 | 459.56 | 481.82 | 91.91±2.07 | 96.36±1.29 |
| River water | 500 | 500 | 464.57 | 486.90 | 92.92±2.63 | 97.38±2.56 |
| Wastewater | 500 | 500 | 460.80 | 474.63 | 92.16±3.53 | 94.93±3.88 |

738 [a] Mean value ± RSD.

739

740

741

742

743

744

745

746

747

748

749

750

751

752

753

754

755

756

757

758

759

760

761

762

763

764

765

766

767

768

769

770

771

772

773

774

775
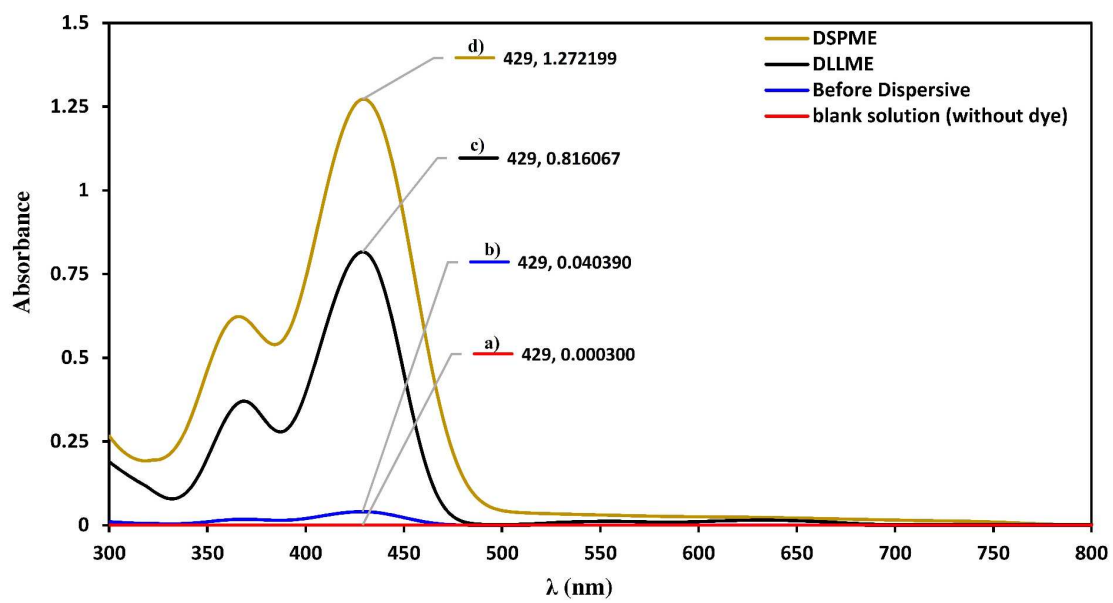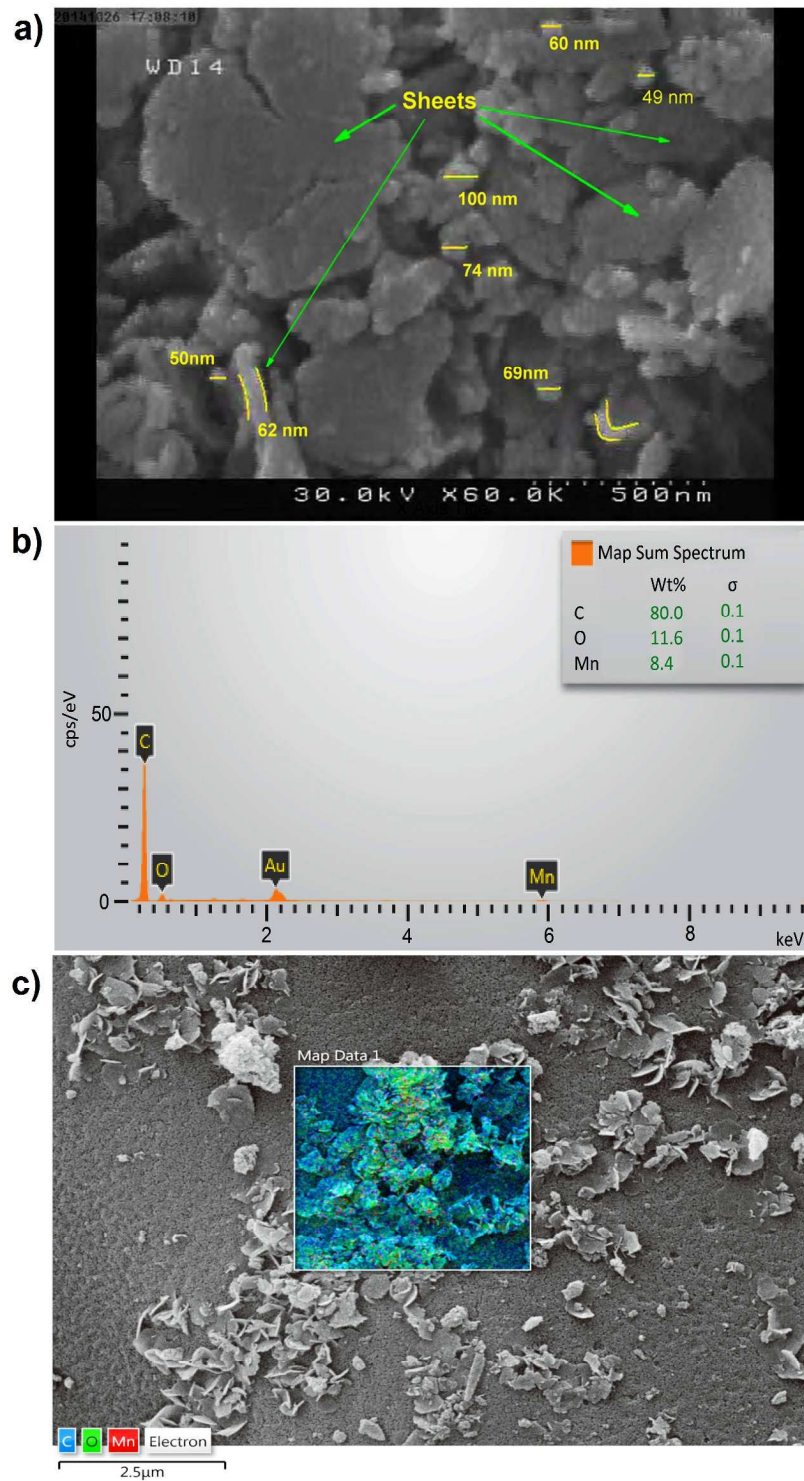
**Fig. 1.**
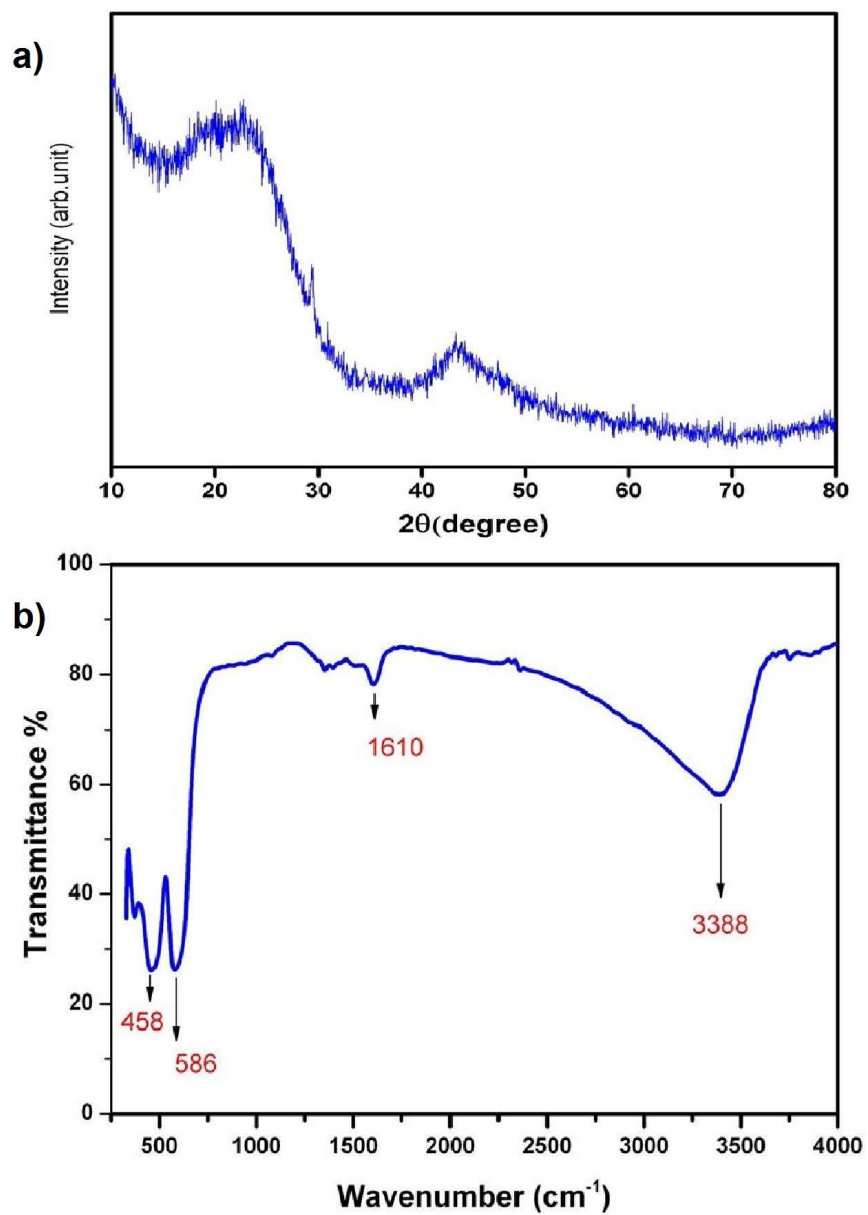
Fig. 3.

782
783
784
785
786
787
788
789
790

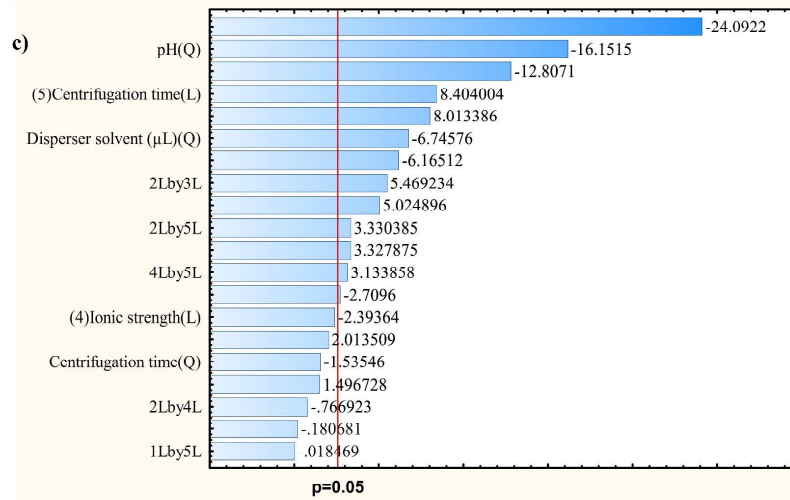791
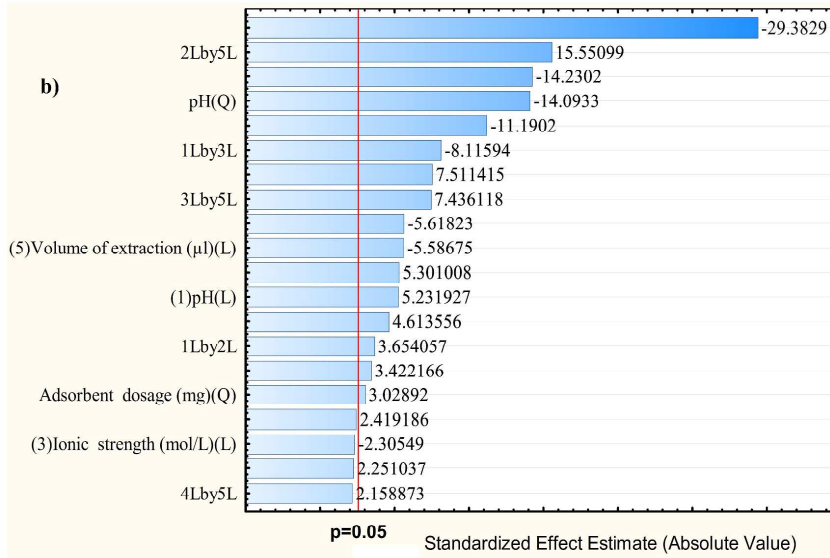792                                                                    **Fig. 4.**
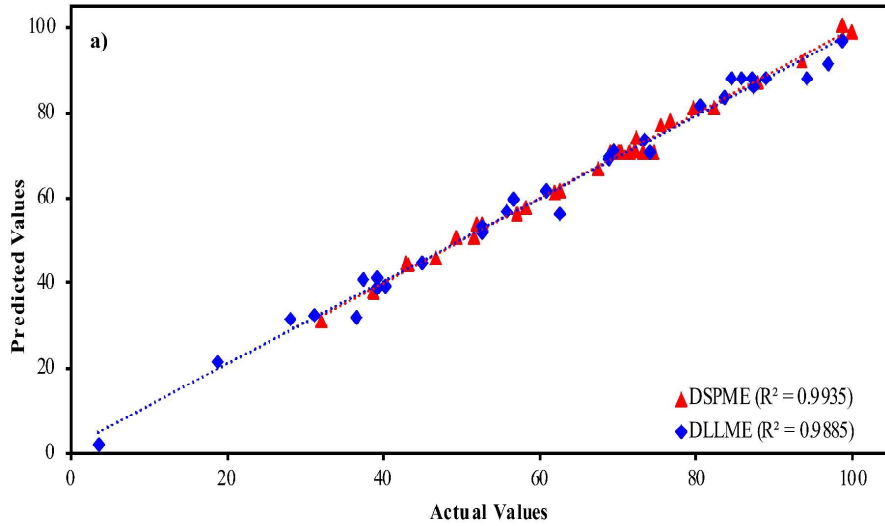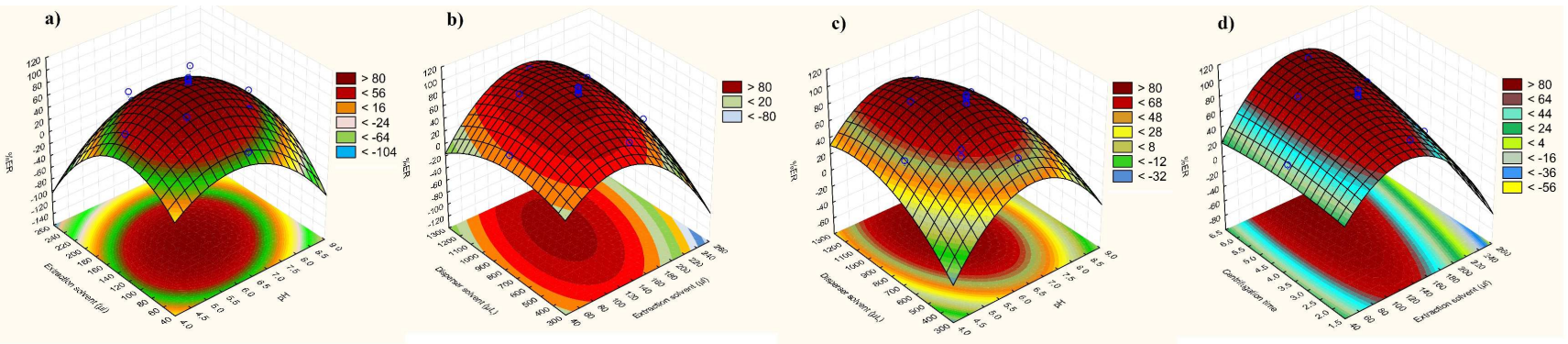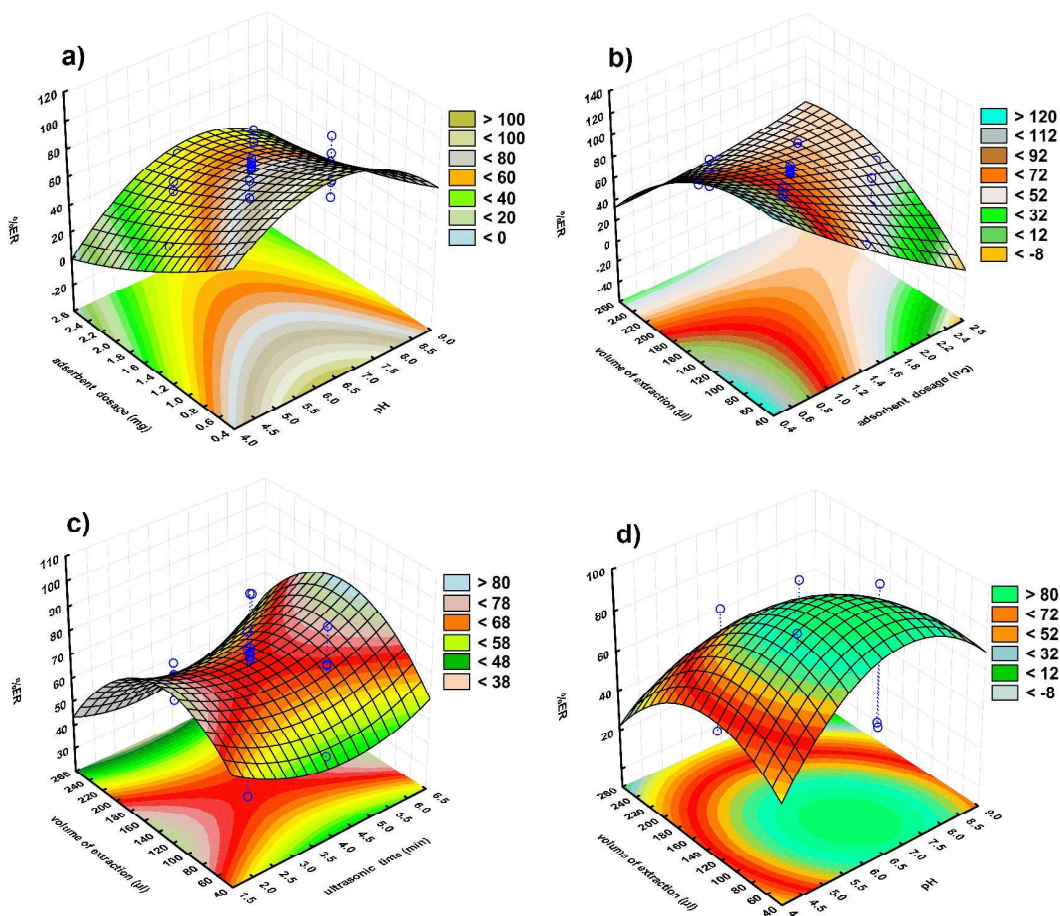793
794

795
796
797
798
799



**Fig. 5.**

800
801
802
803
804
805
806
807
808
809
810
811
812

**Fig. 6.**

813
814
815
816
817
818